Thermal Science and Engineering 2024, 7(4), 8858.
https://doi.org/10.24294/tse8858

Article

Initial analysis and improvements to a stepped piston segregated scavenge engine for ultra-low emission range extender and hybrid electric vehicles

Peter Hooper

Bernard Hooper Engineering Ltd, Wolverhampton WV3 9BU, UK; peter.hooper@bernardhooperengineering.co.uk

CITATION

Hooper P. Initial analysis and improvements to a stepped piston segregated scavenge engine for ultra-low emission range extender and hybrid electric vehicles. Thermal Science and Engineering. 2024; 7(4): 8858.
https://doi.org/10.24294/tse8858

ARTICLE INFO

Received: 29 August 2024
Accepted: 29 September 2024
Available online: 29 November 2024

Abstract: Segregating the scavenging processes from the lubrication methodology is a very effective way of improving two-stroke cycle engine durability. The application of stepped or twin diameter pistons is one such method that has repeatedly shown significantly greater durability over comparable crankcase scavenged engines together with an ability to operate on neat fuel without any added oil. This research study presents the initial results observed from a gasoline/indolene fuelled stepped piston engine ultimately intended for Hybrid Electric Vehicle and/or Range Extender Electric Vehicle application using hydrogen fuelling. Hydrogen fuelling offers the potential to significantly reduce emissions, with near zero emission operation possible, and overcoming the serious issues of range anxiety in modern transport solutions. The low environmental impact is discussed along with results from 1-d Computational Fluid Dynamic modelling. The engine type is a low-cost solution countering the financial challenges of powertrain duplication evident with Hybrid Electric and Range Extender Electric Vehicles.

Keywords: hydrogen vehicle; hybrid electric vehicle; range extender; stepped piston engine; two-stroke cycle

1. Introduction

Battery Electric Vehicles (BEVs) are perceived to be the solution for future low environmental impact transport. However serious problems and challenges remain for BEVs. Range anxiety is a particular problem for adoption of potential new BEV owners as has been discussed by Rauh et al. [1], Reitz et al. [2] and Pevec et al. [3]. The impact on battery life when deep discharge of the vehicle battery system occurs also compounds this problem. Whilst a BEV may have a claimed range, repeated extreme depletion of the state of charge will cause rapid need for replacement of the battery. Furthermore, extreme ambient weather conditions have serious effects on a BEVs useful range adding to the anxiety of BEV users.

BEVs are ideally suited to inner city use and short-range journeys. Development of new battery storage systems is of course a major focus for new BEVs but currently the available range is insufficient for long distance travel. The replacement of EV battery systems is often down played and the fact that the battery pack is a complex device containing rare earth materials means that the cost of changing the battery is prohibitive. The battery system in a 100% electric EV is a large volume unit containing harmful materials as discussed by Sobianowska-Turek et al. [4]. It is not uncommon for EV Batteries to contain, Lithium, Cobalt, Nickel, Manganese and Rare Earth materials as reported by Lipman and Maier [5]. Careful recycling is therefore essential with such materials, not least care in the mining processes to acquire the original raw elements.

A challenging but solvable problem for EV adoption is to use cleaner energy sources. Unfortunately, much of the electricity generated is from fuels that are still carbon based. Coal and gas fired power stations are still predominant in many parts of the World. Essentially, until the transition to clean energy production is achieved, the only thing that EV adoption has achieved is removal of localized tailpipe emissions. The harmful emissions have simply been transferred to the area where the power stations are cited. Unfortunately, the transfer of Oxides of nitrogen (NOx) emission to the coal fired power stations, even with the latest combined cycle technology, is predicted to be higher than can currently be achieved with the latest internal combustion engines as researched by Kalghatgi [6]. It should be stated that some localized harmful emissions do unfortunately still exist with a BEV. The mass of a BEV is appreciably higher than conventional vehicles due to the battery systems. Particulate emissions from BEV tyres and braking systems have been shown to be consequentially higher for BEVs as discussed by Requia et al. [7], Reitz et al. [2] and Klimenko [8]. The new legislation covered by the European Union [9] has imposed regulation of particulate emissions from tyre and braking systems as a source for this very reason.

Smarter thinking is required to transition the World into a cleaner future. Considering BEVs as the only answer is unwise at the present time. Range Extender Electric Vehicles (RE-EVs) and Hybrid Electric Vehicles (HEVs) have a strong part to play as the cleaner energy future develops. RE-EVs and HEVs require smaller batteries than comparable 100% electric BEVs. This means that less material and battery volume is required. There are challenges due to powertrain duplication but if low-cost engine technology can be successfully applied then the increased cost caused by the duplicity can be countered. Furthermore, if clean fuels such as hydrogen [10] or e-fuels as discussed by Ravi et al. [11,12] are available for the onboard combustion engine of the HEV or RE-EV then any negative environmental impact from that source of the vehicle can be minimized or in some cases even eliminated.

If the negative impact of increased vehicle mass is to be addressed by the use of HEVs and RE-EVs then the engine system providing the recharging facility needs to be ideally of minimum mass. Dedicated spark ignition gasoline power plants have been considered for RE-EVs as evidenced by the research of Bassett et al. [13]. Advanced methodologies have also been explored for compression ignition diesel engines for HEVs in terms of engine operational parameters (variable compression ratio and injection timing), material tribological considerations [14–16] and use of lubricant nanoparticles to reduce friction and emissions [17]. Research has also focused on improving the emissions of compression ignition engines via natural gas operation [18]. In order to minimize internal combustion engine mass, the two-stroke cycle engine offers significant advantages over the four-stroke engine. Two-stroke engines have been developed to operate on hydrogen. The first engine to be developed for hydrogen fuel in 1860 was a two-stroke engine, based on the research of Etienne Lenoir [19], who generated the fuel by water electrolysis. More recent hydrogen two-stroke engine developments are exampled by the research of Furuhama and Kobayashi [20] and via the work of Caprioli et al. [21], Mattarelli et al. [22] and Volza et al. [23].

Hydrogen offers significant advantages over conventional fuels used within internal combustion engines. Notwithstanding the fact that hydrogen has to be created if it is to be used as a fuel, the fact that it contains no carbon means that the historic problematic emissions of unburned hydrocarbons, carbon monoxide and carbon dioxide are removed from the combustion challenge. The range of flammability of hydrogen is wider than that achievable with gasoline fuel as discussed by Karim [24]. This essentially means that lean air: fuel mixture operation is possible with hydrogen. Furthermore, hydrogen flame speeds are faster than those observed with gasoline as has been discussed by Verhelst and Turner [25], Shinde and Karunamurthy [26], Cracknell et al. [27] and Onorati et al. [28].

Oxides of nitrogen (NOx) form the significant noxious gas emission that still remains with internal combustion of hydrogen. Two-stroke engines have repeatedly demonstrated low NOx emissions on gasoline [29,30] and diesel fuels when compared with comparable four-stroke engines and therefore present an attractive starting place in order to minimize this remaining emission group. Indeed, taking advantage of the wide flammability range of hydrogen and hence possibilities for lean air: fuel mixture operation means that the NOx levels can be reduced to very low levels. Unfortunately, conventional crankcase scavenged two-stroke engines suffer from relatively low durability due to their inherent design configuration and construction. The simplest forms of the crankcase scavenged two-stroke engine mix oil with the fuel or use a precision metering pump to supply the lubricant. All of this supplied oil is consumed on a total loss basis, creating significant negative impact on their emissions characteristics. However, a two-stroke engine that has repeatedly shown significantly higher durability, comparable with four-stroke engine standards, is offered by the stepped piston engine. This engine design operates on neat fuel with no added oil completely separating the lubrication system from the air scavenging path, thereby overcoming the problems of conventional crankcase scavenged two-stroke engines. The critical areas of the engine requiring lubrication such as the piston and rings are lubricated discretely with metering holes allowing oil from the sump to reach the crucial areas strategically. This has resulted in significant reductions in oil consumption when compared with conventional crankcase scavenged engines [31].

Historically achieving low emission levels with conventional two-stroke engines has been difficult. This is due to the relatively high oil consumption of conventional engines and the fact that short-circuiting of the incoming air: fuel charge into the exhaust can occur during the open port phase of the cycle around bottom dead centre. However, the advent of fuel injection directly into the combustion chamber has shown significant improvements in emissions reduction as demonstrated by the research of Duret et al. [32], Schlunke [33], Shawcross et al. [34] and more recently via the research of Turner et al. [29] and Blundell et al. [30]. Essentially direct injection (DI) allows fuel delivery to be achieved without short-circuiting, thereby greatly reducing emissions. Two-stroke engines have always exhibited low NOx emission even without DI due to the low temperature and pressure of two-stroke combustion when compared with four-stroke engines. The stepped piston engine also retains the two-stroke cycle characteristic of emitting low NOx emission [35,36].

Hydrogen fuel operation of engines has been reported to create corrosion problems as discussed by Stępień [37]. Crankcase scavenged two-stroke engines utilize the underside of the piston as a scavenge pump. Corrosion issues would be very problematic to such engines due to the fact that the crankcase houses crucial bearings and other components that could suffer from exposure. Furthermore, crankcase scavenged engines are not ideally suited to gaseous fuel operation. For this research study a segregated scavenge two-stroke engine is required and the proposed solution is offered by an engine using two diameter or stepped pistons [35]. Stepped piston engines have previously shown good results operating on gaseous fuels as indicated from a 500 cm^3 stepped piston engine loaned to British Gas in the UK for experimentation using natural gas as a fuel. Conclusions from that work suggested that future hydrogen operation could be beneficial.

This paper builds upon prior experimental and 1-d computational fluid dynamic (CFD) work, investigating improvements to the CFD models to better correlate with the experimental stepped piston engines and initial consideration of the possible benefits of hydrogen fuel operation.

2. Materials and methods

2.1. Fuel properties

Properties for the fuels relevant to this research study are presented for reference in **Table 1**.

Table 1. Physical and chemical fuel properties.

Property		**Hydrogen**	**Indolene**	**95RON Gasoline**
Research octane number		130	96.7	95.6
Lower heat value	(MJ/kg)	121	43.1	43.2
Flammability limits	(% by vol)	4–75	1.1–6.0	1.2–6.0
Stoichiometric air: fuel ratio AFRs		34.3	14.7	14.7
Composition (atoms per molecule)				
Carbon		0	7.8	~8
Hydrogen		2	13.2	~15
Oxygen		0	-	-
Nitrogen		0	-	-

2.2. Stepped piston segregated scavenge engines

The engine used as the basis of the study is a twin cylinder engine of 290 cm^3 swept volume, manufactured by Bernard Hooper Engineering Ltd, UK. The engine is effectively half of a SPV580 unmanned aerial vehicle (UAV) engine [35,38] using two cylinders instead of the four employed in the larger engine. The two-cylinder engine is designated UMA290 [39]. The V-4-cylinder SPV580 UAV engine has been developed to produce in excess of 61 kW/litre at 5250 rpm (gasoline version) to date [36,40]. For reference a production version of the parallel twin cylinder UMA290 engine can be seen in **Figure 1**.

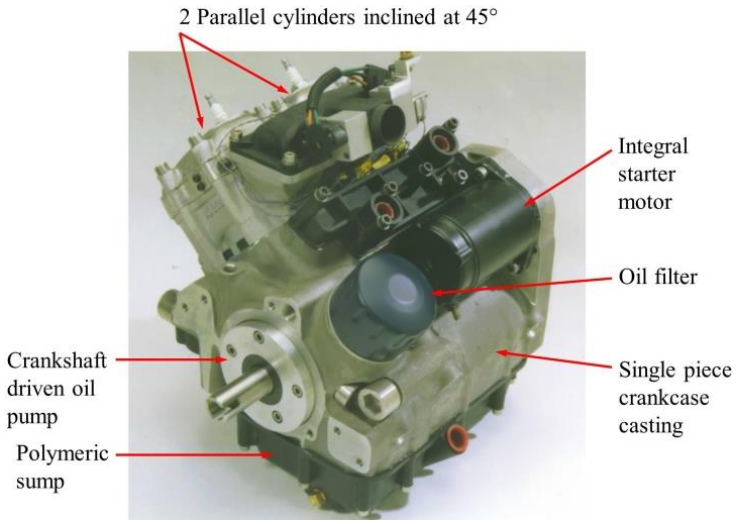

Figure 1. UMA290 290 cm^3 twin cylinder stepped piston engine.

The method of operation of the UMA290 is described by the operating principle of the stepped piston crossover system (SPX system) in **Figure 2**.

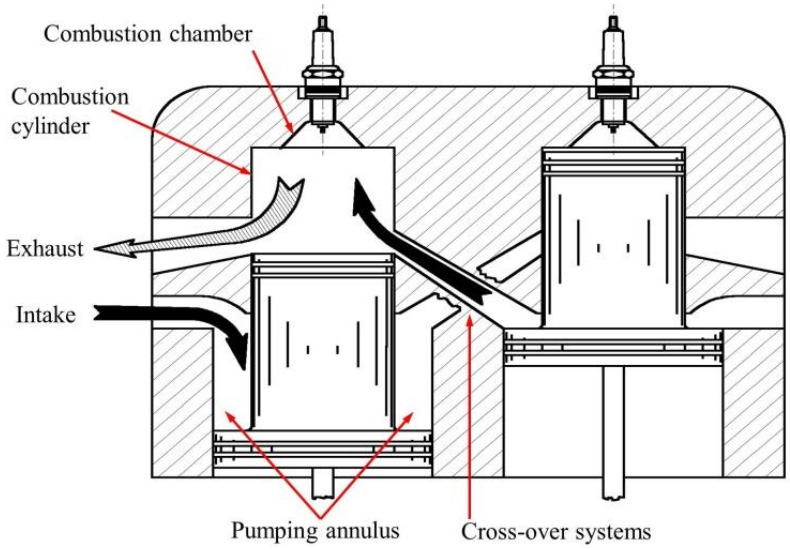

Figure 2. SPX engine operating principle (schematic representation of cross-over).

The SPX crossover system is employed on the majority of the multi-cylinder stepped piston engines such as the SPV580 and UMA290. It is however quite possible for single- and three-cylinder configurations to function. As can be observed from **Figure 2**, the cylinders of the UMA290 function in pairs. The air charge is inducted by the larger diameter or pumping part of the one-piece piston via a non-return or reed valve as are commonly employed on crankcase scavenged two-stroke engines. With reverse flow prevented the charge passes into the crossover system, allowing transfer of the charge to pass to the relevant paired cylinder. The charge enters the combustion cylinders via transfer ports. Combustion is similar in many ways to Schnürle loop scavenged engines. After combustion the spent gases are scavenged from the upper cylinders via exhaust ports. It is possible to design stepped

piston engines as uni-flow configurations, using exhaust poppet valves in the cylinder head, however this naturally compromises the compactness of the power plant.

The stepped piston engine offers key advantages over normal two-stroke and four-stroke engines. A significant advantage when compared with conventional crankcase scavenged two-stroke engines lies in the provision of total separation of the lubrication and charge air induction processes. The lubrication system is very similar to that commonly found in four-stroke engines, being completely filtered and recirculatory, using plain hydrodynamic shell bearings. Two-stroke engines that use crankcase scavenging typically use rolling element bearings which are a significant cost and noise source giving detrimental NVH issues. Furthermore, when considering gaseous fuel operation more specifically, the isolation of combustion blow-by gases from the crankcase and therefore contamination of bearings, surfaces and lubricant, that create problems in conventional two and four-stroke engines is eliminated. Hydrogen fuelled engines have been reported to cause internal corrosion issues within engines as discussed by Stępień [37]. The isolation methods available within the segregated design of the stepped piston engine could offer significant advantage with respect to such corrosion problems.

A partial cross-sectional general arrangement of the UMA290 engine is presented in **Figure 3**.

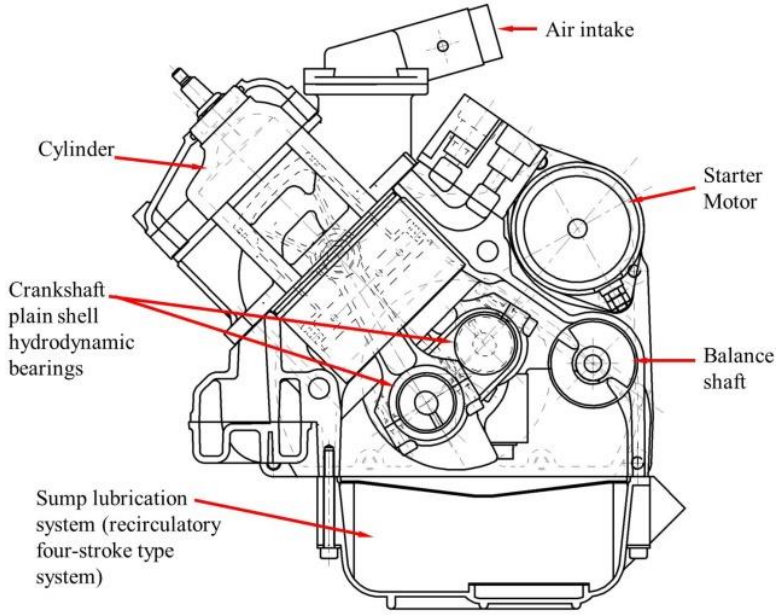

Figure 3. General arrangement of the UMA290 twin cylinder stepped piston engine.

The combustion cylinders of the engine shown in **Figure 3** each have a swept volume of 145 cm^3. The cylinders are of individual unit design with the pumping cylinders housed inside the crankcase. The crossover systems also form part of the crankcase. **Figure 4** displays a comparison of the port belt area of a conventional Schnürle loop scavenged engine and the same swept volume unit if scavenged by stepped pistons.

The cylinders are aluminium (Al Si7 Mg0.5) with both bores coated with a nickel silicon carbide coating (GILNISIL) applied by Gilardoni Vittorio S.r.l., Italy.

The pistons are low pressure die-cast using a high silicon aluminium alloy (Al Si18 Cu Mg Ni).

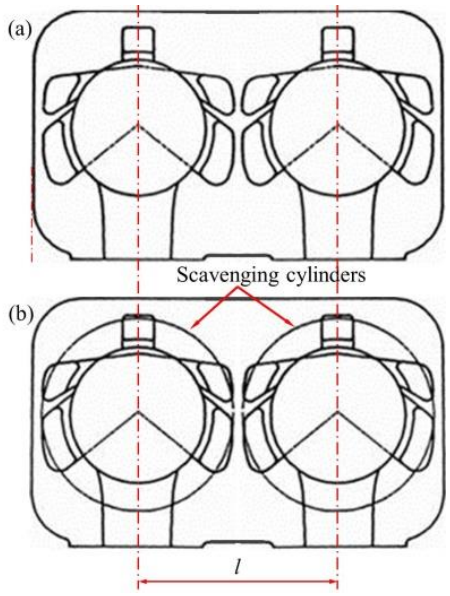

Figure 4. Two-stroke engine port layout comparison using identical bore diameter and swept volume **(a)** Schnürle loop scavenge; **(b)** Schnürle loop stepped piston segregated scavenge engine.

Naturally a stepped piston, by virtue of its design, will possess a greater plan profile than a conventional single diameter piston displacing the same swept volume. However, if we consider cylinder centre distance, *l*, it can be seen from close examination of **Figure 4** that the larger diameter pumping piston does not actually increase the engine cylinder spacing when compared with a conventional loop scavenged engine. The space required for the conventional engine's transfer ports typically expands the cylinder centre distance, *l*.

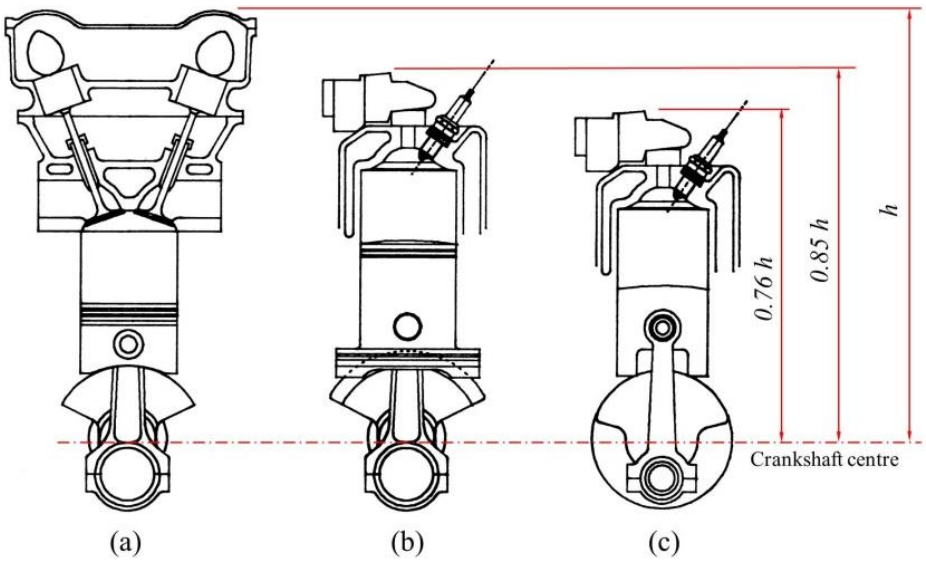

Figure 5. Engine height comparisons with identical swept volumes **(a)** DOHC four-stroke; **(b)** stepped piston; **(c)** conventional crankcase scavenged two-stroke engines.

The analysis shown in **Figure 5** is based upon identical cylinder swept volumes for each engine type. If the operational maximum power speed is also set as a constraint, the four-stroke engine would have to be larger to achieve the same power output. From **Figure 5** it can be seen that the stepped piston engine is smaller than the four-stroke engine but not quite as compact as a conventional crankcase scavenged two-stroke engine in terms of engine height.

The UMA290 engine was mounted on a dynamometer to establish baseline experimental data using 95RON gasoline as shown in **Figure 6**.

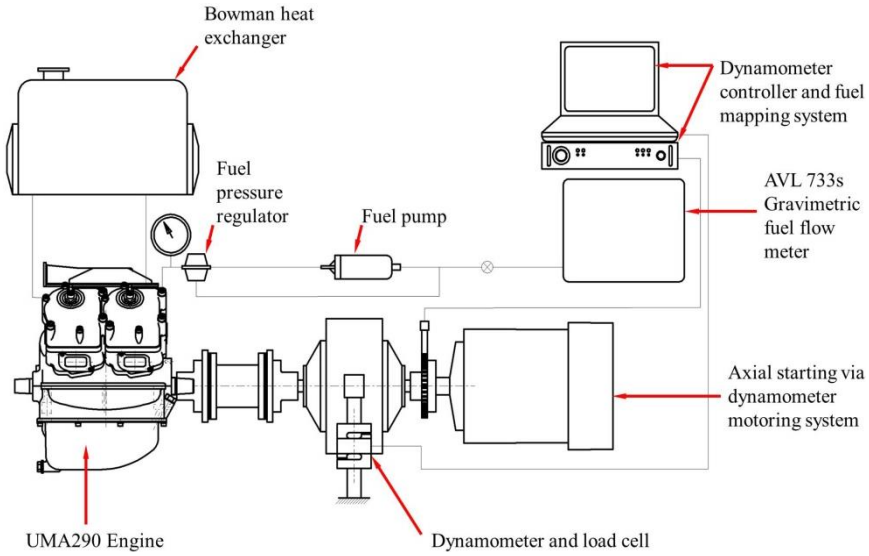

Figure 6. Schematic of UMA290 engine dynamometer test facility.

Experimental test results secured from the UMA290 engine were recorded using a Froude eddy current dynamometer equipped with a load cell. Fuel injector pulse width and ignition timing was mapped using a computer driven interface linked to the writable engine electronic control unit. A Hall effect sensor provides timing reference from the engine crankshaft and subsequent injector sequencing with timing variable via the PC interface. The system also has air temperature, coolant temperature, barometric pressure, throttle position and air mass flow sensors. The fuel flow was monitored using an AVL 733s gravimetric fuel balance. All test data reported in this paper was recorded at full load wide open throttle operating conditions at stoichiometric air: fuel ratio.

2.3. Modelling methodology

Details of the design of the UMA290 and a comparable four-stroke engine of 374 cm^3 capacity are listed for reference in **Table 2**.

Table 2. Engine design specification.

Engine		**UMA290**	**4s 374**
Operating cycle		2-stroke	4-stroke
Swept volume	(cm^3)	290	374
Scavenging system		Stepped piston	Naturally aspirated
Pump compression ratio		1.5	-

Table 2. (*Continued*).

Engine		**UMA290**	**4s 374**
Cylinders		2	2
Bore	(mm)	62	62
Stroke	(mm)	48	62
BMEP	(bar)	7.3	12.1
Maximum BMEP speed	(rpm)	4500	4000
Compression ratio		6.2:1	10:1
Specific power	(kW/l)	58.4	60.7
Maximum power speed	(rpm)	5000	6000

(All performance data is at full load stoichiometric wide open throttle operating conditions)

2.3.1. Computational engine modelling

The Computational fluid dynamics (CFD) models adopted a parent-child simulation where the boundary conditions and flow data are exchanged between the models. The pumping cylinders and associated inlet passageways form the basis of the parent model. The child model comprises the crossover systems, combustion cylinders and exhaust system of the UMA290 engine. The 1-d CFD code, WAVE (version 2023.1), developed by Realis Simulation/Ricardo [41] was used for all simulations reported in this research study. Statistical methods developed by Gajević et al. [42] were used in order to process test results. The UMA290 parent and child stepped piston model layouts are shown in **Figures 7** and **8** respectively.

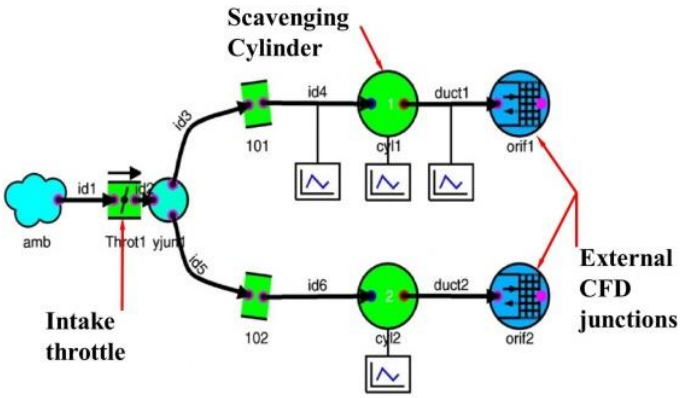

Figure 7. UMA290 Engine 1-d CFD model (parent model).

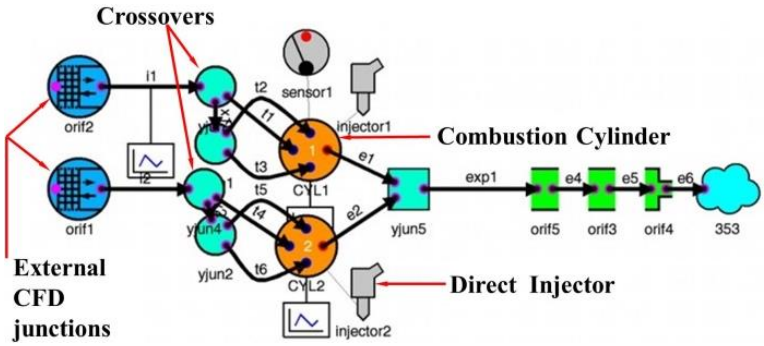

Figure 8. UMA290 Engine 1-d CFD model (child model).

Boundary conditions and mass flow data is exchanged between the parent and child models via the external CFD junction.

The WAVE model built to establish data from a comparative 374 cm^3 twin cylinder four-stroke engine, reflecting the data shown in **Table 2**, is displayed in **Figure 9**.

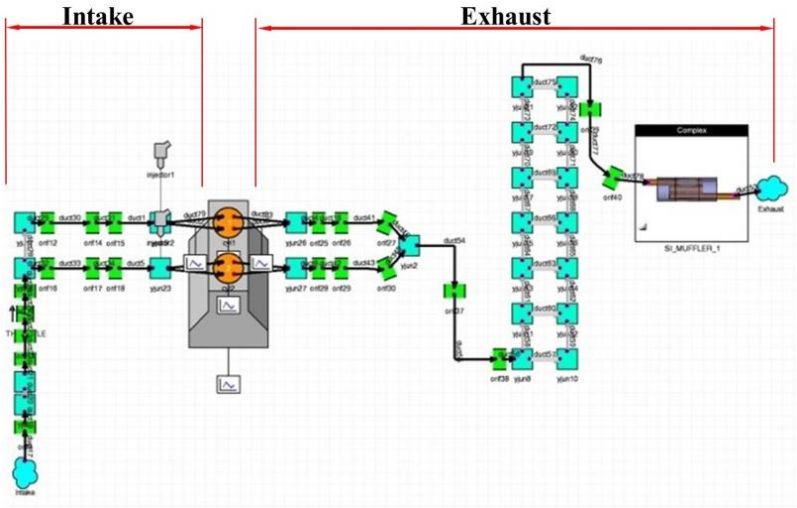

Figure 9. 374 cm^3 Four-stroke cycle engine 1-d CFD model.

2.3.2. Model theory

The construction of the WAVE models is essentially a collection of interconnected pre-defined elements of ambients, throttles, ducts, junctions and valves ultimately linking to combustion cylinders, and in the case of the UMA290, pumping cylinders. Each element is user defined in terms of dimensions, surface roughness and thermodynamic/heat transfer properties. The engine passageways are represented by ducts and are discretized as predefined elemental cells. At the centre of each individual cell calculations of instantaneous pressure and temperature are made whilst at the boundary points of each cell flow velocity and mass flowrate are computed. Equations (1)–(3) are used to compute conservation of mass, energy and momentum respectively:

$$\frac{\partial \rho}{\partial t} + \frac{\partial (\rho u)}{\partial x} = 0 \tag{1}$$

$$\frac{\partial (\rho u)}{\partial t} + \frac{\partial (\rho u^2 + P)}{\partial x} = \frac{\partial}{\partial x}\left(\frac{4\mu}{3}\frac{\partial}{\partial x}\right) \tag{2}$$

$$\frac{\partial (\rho e_T)}{\partial t} + \frac{\partial (\rho u e_T + Pu)}{\partial x} = \frac{\partial}{\partial x}\left(\frac{4}{3}\mu u\frac{\partial u}{\partial x} + k\frac{\partial T}{\partial x}\right) \tag{3}$$

Two-stroke engines require a means of inlet flow control. These can be one or more of the following:

1) Piston-port control
2) Rotary valve
3) Reed valve

Piston-porting is essentially control of the inlet flow via the engine's piston

passing over the inlet ports at the correct required time. Rotary valves can be disc or cylindrical elements driven by the engine allowing synchronized opening and closing of the inlet passages supplying the engine. The final choice is the reed valve. This is an automatic non-return valve designed with petals or reeds that are light enough to respond to the pressure drop across the valve block. Combinations of the above have been successfully applied such as the application of reed valves and piston-port control by Yamaha via the research of Hata et al. [43].

The UMA290 engine uses two individual reed valve blocks located within the inlet tract of each pump cylinder. However stepped piston engines, developed to date, have employed each of the three possible forms of inlet control. The reed valves employed comprise two sets of interconnected phenolic resin petals located on each side of a triangular prism shaped reed block. Within WAVE the reeds of the reed valves are modelled as light cantilevers based upon the reed's natural frequency and fundamental modes of vibration (lower order modes). The theory can be examined for reference via the research of Hinds [44] and Morrison and Crossland [45].

After passing through the reed valves the air is drawn into the individual pumping cylinders. The reed valves prevent reverse flow and the charge is passed to the external CFD junctions shown in **Figure 7** for exchange to the relevant linked junction in **Figure 8**. The crossover is represented by defined ducts replicating the passageways used that link to the cylinder transfer ports. Once within the cylinder the combustion is modelled using a Wiebe function as defined by the formula shown in Equation (4).

$$x(\theta) = 1 - exp\left[-\left[\frac{c(\theta - \theta_0)}{\Delta\theta_b}\right]^{-b}\right] \tag{4}$$

Equation (4), was developed by Wiebe [46] to compute the mass fraction burned, $x(\theta)$, as the combustion process incrementally progresses. Constants, b and c, are selected in order to replicate the actual combustion profile. It is possible to generate a representative Wiebe function from actual engine cylinder pressure data. However, in the absence of any available data for the UMA290 the prior research of Heywood and Sher [47] was explored. Above the crown of the combustion piston, the stepped piston engine is similar in many ways to the environment found above the piston crown of a crankcase scavenged two-stroke engine. Through analysis of crankcase scavenged two-stroke engines, values of b = 5 and c = 3 to 3.2 were derived by Sher [48]. These values have been used in order to generate the Wiebe function within the WAVE models developed within this research study. The prior research of Heywood and Sher [47] and Sher [48] considered gasoline fuel. This has been used to try to improve the correlation of the indolene fuelled stepped piston two-stroke models.

One of the biggest variables in engine modelling is often found in the representation of how heat transfer occurs within the actual engine and its representative model. Away from the cylinder the Colburn analogy [49] is used to compute the coefficient of heat transfer, h, as defined by Equation (5).

$$h = \frac{C_f}{2}\rho U c_p Pr^{-\frac{2}{3}} \tag{5}$$

In the area of the combustion cylinder the well-established analysis developed by Woschni [50] was used where the coefficient of heat transfer, *h*, is computed from Equation (6).

$$h = 0.0128\, D^{-0.2} P^{0.8} T^{-0.53} {v_{ch}}^{0.8} C_m \tag{6}$$

A key input to Equation (6) is the scaling factor, C_m. This value defines the surface area ratio of the piston crown and combustion chamber profile. A value of $C_m = 1$ defines the piston as a flat top or a flat combustion chamber. C_m is therefore set to reflect the increased surface area of the actual piston and/or cylinder head profile. For the UMA290 $C_m = 1.267$. The characteristic gas speed, v_{ch}, equates to the engine mean piston speed. P and T are the instantaneous cylinder pressure and temperatures respectively.

Engine friction is accounted for in the WAVE models via inputs to the correlation developed by Chen and Flynn [51] and reproduced for reference in Equation (7).

$$p_f = c_1 + c_2(p_{max}) + c_3\left(N\frac{s}{2}\right) + c_4\left(N\frac{s}{2}\right)^2 \tag{7}$$

Data from motored friction tests or Morse tests (in the case of the UMA290) can be used as input values influencing the computation of friction mean effective pressure, p_f, in Equation (7). Essentially the values of constants, c_1 to c_4, are adjusted until the FMEP replicates the data recorded from the real engine. The engine stroke is defined by the variable, s, in Equation (7), the engine speed is represented by N and p_{max} is the maximum cylinder pressure.

In order to predict the onset of combustion knock within the models, the induction time correlation developed by Douaud and Eyzat [52] is used. At each time step the knock intensity is reported, flagging that knock is occurring during the model runs. The induction time or ignition delay, τ, is computed at each time step in accordance with the formula shown in Equation (8).

$$\tau = 0.01869 A_p \left(\frac{O_N}{100}\right)^{3.4017} {p_{cyl}}^{-1.7} exp\left(\frac{3800/A_T}{T_{unb}}\right) \tag{8}$$

The octane number of the fuel, O_N, is a critical input value for Equation (8) and is defined for the fuel selection within the WAVE model. The variables A_p and A_T are user defined in relation to activation temperature. The cylinder pressure at the relevant point in the cycle is defined by p_{cyl} and the temperature of the unburned gas fraction within the cylinder is defined by T_{unb}. The user is informed when knock is detected within the model. The induction time, τ, reduces as the cycle progresses with a corresponding increase in temperature within the unburnt fuel mixture. Auto ignition within the model will be evident when the condition of Equation (9) reaches unity.

$$\int_{t_0}^{t_i} \frac{d\tau}{\tau} = 1 \tag{9}$$

3. Results and discussion

Results

All experimental test data was corrected for standard atmospheric conditions to SAE Standard J1349 [53]. Dynamometer tests were all performed with 95RON gasoline. WAVE modelling was performed via optimisation methods for both the stepped piston engine (UMA290) and four-stroke engine (4s 374) models. The UMA290 models are further developments of prior work [36]. This development work focused on indolene fuel. Indolene is a reference fuel similar to gasoline. Gasoline varies around the world, and indeed from state to state in the USA. Indolene is a reformulated form of gasoline with additives to stabilize the fuel, thereby providing better repeatability than standard pump gasoline.

Engine performance data is compared for UMA290 engine and four-stroke engine models in **Figures 10** and **11**. No combustion knock was observed for any of the model runs using indolene presented within this paper. For reference in **Figures 10** and **11**, dynamometer 95RON gasoline test data from an experimental UMA290 engine is shown.

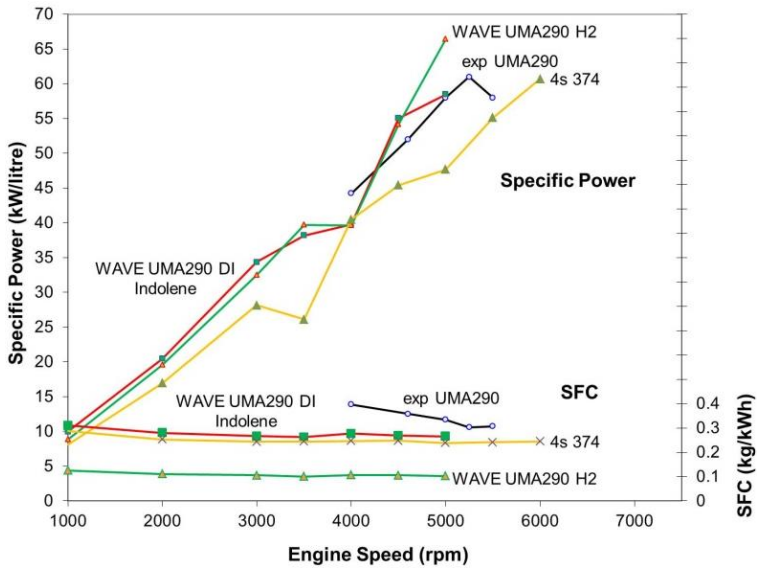

Figure 10. Comparison of specific power and specific fuel consumption using 95RON Gasoline or Indolene as a fuel.

The WAVE modelling so far has indicated an improved maximum specific power for the UMA290 stepped piston engine of 58.4 kW/litre at 5000 rpm. The equivalent experimental stepped piston engine output is currently up to 61.1 kW/litre at 5250 rpm [35] operating on 95RON gasoline. The improvement in the models using indolene can now be seen to be providing closer correlation than was achieved in previous modelling results. The four-stroke 374 cm^3 engine (designated 4s 374 in **Figure 10**) was modelled to achieve a specific output of 60.7 kW/litre at 6000 rpm.

The specific fuel consumption results have indicated a minimum SFC of 0.262 kg/kWh at 3500 rpm and 0.265 kg/kWh at 5000 rpm. The experimental UMA290 engine achieved 0.303 kg/kWh during dynamometer tests at 5250 rpm. Modelling of the four-stroke comparator 4s 374 engines indicated a minimum of 0.240 kg/kWh at

5000 rpm.

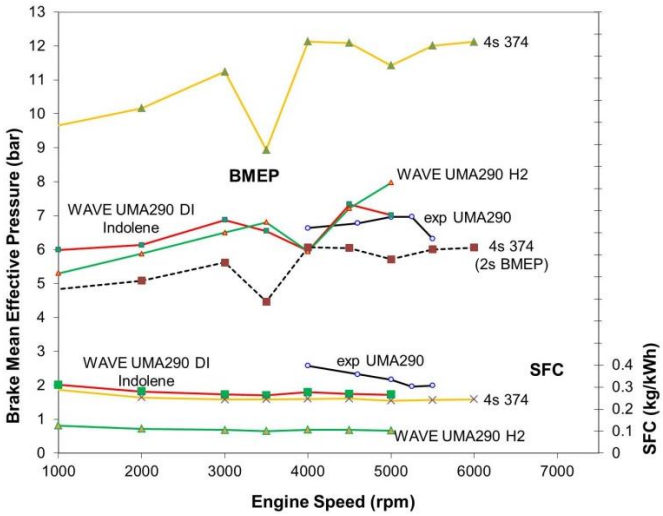

Figure 11. Comparison of modelled brake mean effective pressures using 95RON gasoline or indolene fuel.

In terms of brake mean effective pressure, the four-stroke engine maximum performance equates to a BMEP of 12.13 bar at 4000 rpm using indolene fuel. The UMA290 engine's maximum BMEP can be seen to occur at 4500 rpm with a magnitude of 7.34 bar. During dynamometer testing the experimental UMA290 achieved a level of 6.97 bar at 5250 rpm.

The dashed line shown in **Figure 11** shows the equivalent two-stroke BMEP levels for the 4s 374 engine. Inflection points can be observed for both engine models in **Figures 10** and **11**. These appear at 3000 rpm for the four-stroke 4s 374 engine and at 4000 rpm for the UMA290 engine. Both models were subject to optimisation efforts in order to try to investigate these inflections. This work resulted in making them less pronounced but it was not possible to remove them without significant effect on the maximum power level.

In **Figure 12** modelled cylinder pressure for the indolene fuelled WAVE models are displayed at 3000 rpm.

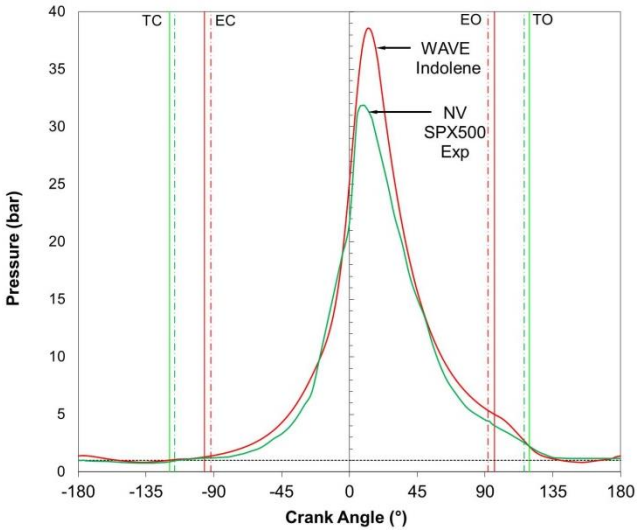

Figure 12. Comparison of modelled cylinder pressures using gasoline and indolene fuels.

A stepped piston motorcycle and single cylinder industrial engines were developed at Norton Villiers via the research of Hooper and Favill [54]. The NV SPX500 Exp curve presented in **Figure 12** is taken from experimental test engine data from that research. Added data shown in **Figure 12** has been taken from the WAVE models created during the more recent research study. The port timings are indicated by the vertical TC, EC, TO and EO lines, denoting the exhaust (E) and transfer (T) port closure (C) and opening (O) points.

Figures 13 and **14** display gas dynamic and mass flow computations for the UMA290 engine models. In each case data from the current study are compared with earlier research data.

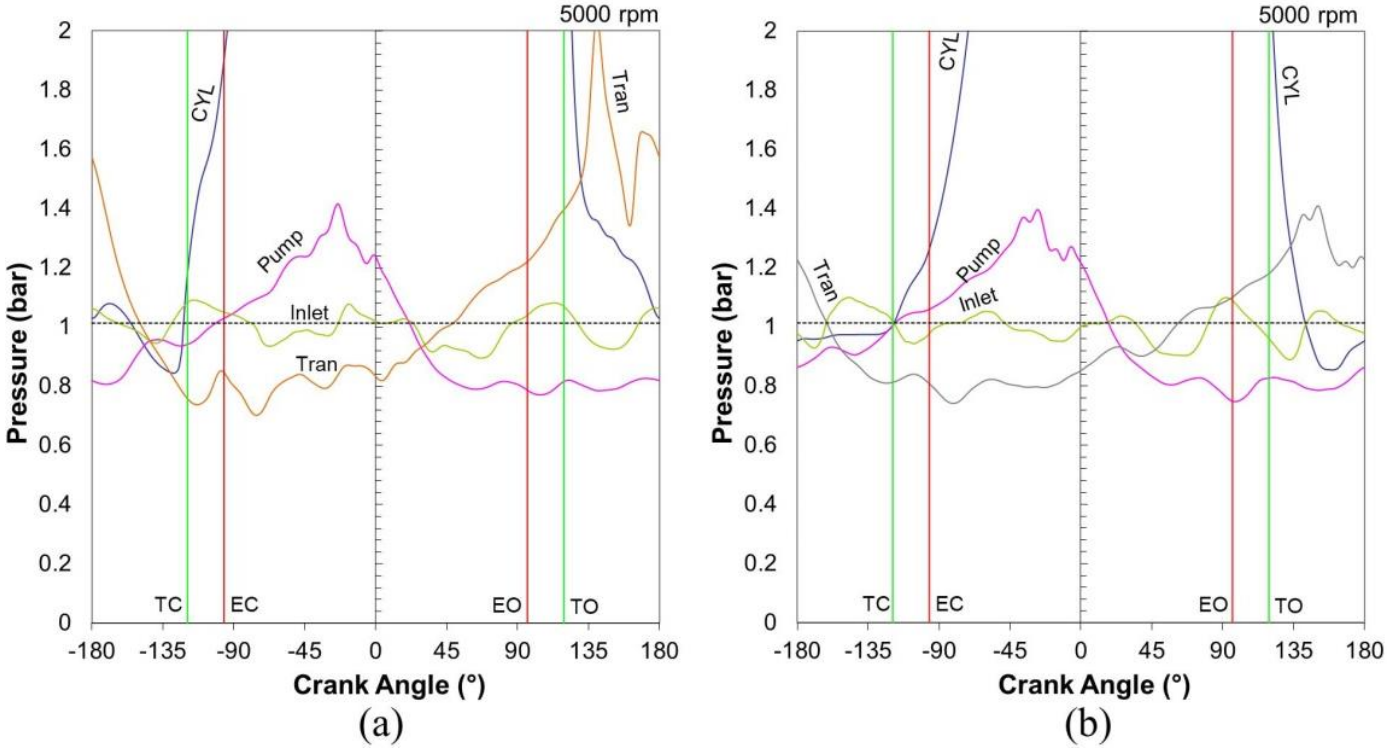

Figure 13. Gas dynamic analysis of UMA290 engine operating on indolene **(a)** UMA290 (2024); **(b)** UMA290 (2017) [36]–5000 rpm.

Data from the recent research study is shown in **Figure 13a** with the model data from prior work shown for comparison in **Figure 13b**. The higher rate of cylinder pressure rise can be seen in **Figure 13a**. Also, the greater transfer port pressure can also be seen as a significant improvement over **Figure 13b**. This higher pressure is evident in the indolene fuelled models and explains the increased performance achieved since the earlier research reported.

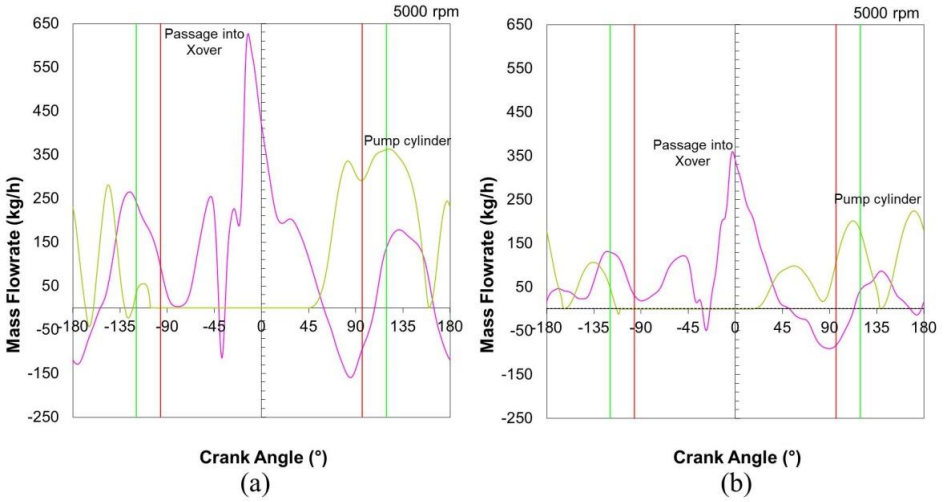

Figure 14. Mass flow through inlet and crossover systems of UMA290 **(a)** UMA290 (2024); **(b)** UMA290 (2017) [36]–5000 rpm.

The mass flow data shown in **Figure 14a** relates to the most recent research with the earlier model data being displayed in **Figure 14b**. Whilst a greater level of negative flow can be seen in **Figure 14a** when compared with **Figure 14b**, the overall increase in positive mass flow towards the combustion cylinders is also clearly evident. As for the increased pressures seen in **Figure 13a**, the improvement in mass flow of the air charge supports the observed performance improvements achieved in the current research using indolene fuels.

Actual pumping cylinder pressure data from other stepped piston engines is presented in **Figure 15** to provide a cross comparison with the WAVE model data recorded from the indolene fuelled models.

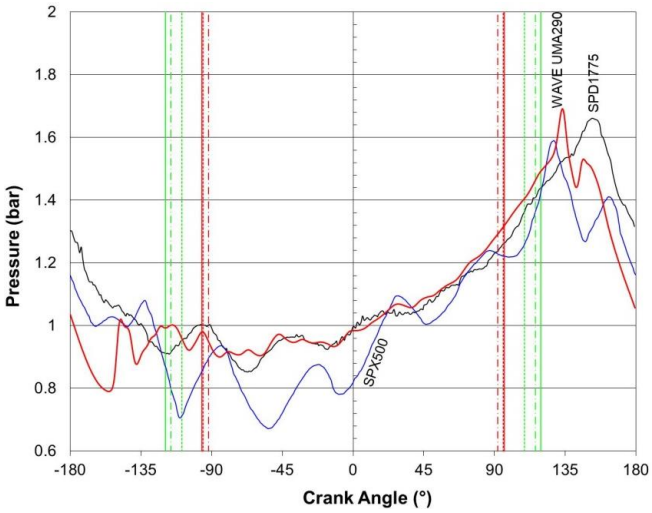

Figure 15. Pumping cylinder pressure for stepped piston prototype engines and WAVE model data.

The experimental engine data shown in **Figure 15** was recorded from an SPX500 engine and an SPD1775 engine. The SPX500 was the engine developed for the Norton Wulf motorcycle. The data was recorded at Norton Villiers during development of the engine. The SPD1775 is a 4-cylinder compression ignition

stepped piston engine of 1775 cm^3 swept volume. This engine data, recorded at 3000 RPM, is included purely for comparative purposes. All of the engines shown in **Figure 15** use reed valve-controlled induction systems. The transfer and exhaust port timings are shown for reference in **Figure 15** for the UMA290 (solid lines), SPX500 (chain dash lines) and SPD1775 (dashed lines).

4. Discussion

The UMA290 has been the subject of previous research studies [36]. The work in this phase of research has improved the performance of the original indolene models, improving the correlation with the real engine prior to future planned work using hydrogen fuel. The maximum specific power at 5500 rpm was 49 kW/litre which was below the performance levels observed during dynamometer testing of the experimental UMA290 engine using 95RON gasoline. Observations from the latest research reported here has achieved a higher maximum specific power level at 5000 rpm of 58.4 kW/litre. Despite this 24.3% performance improvement the results are still lagging the experimental engines (achieving 61.1 kW/litre at 5250 rpm) by 4.6%. The 374 cm^3 twin cylinder four-stroke engine achieved a modelled output at 6000 rpm equating to 60.7 kW/litre.

The comparative brake mean effective pressures showed a maximum BMEP of 12.13 bar at 4000 rpm for the 374 cm^3 four-stroke engine, whilst the UMA290 maximum BMEP was observed at 4500 rpm with a level of 7.34 bar using indolene. It should of course be remembered that the UMA290 is a two-stroke cycle engine. The SPV580 stepped piston engine which is in simple terms two UMA290 units has been tested on 95 RON gasoline to a maximum BMEP of 6.97 bar at 5250 rpm.

Specific fuel consumption data recorded during the current research has indicated a minimum WAVE modelled full load SFC of 0.262 kg/kWh at 3500 rpm using indolene WAVE models. Closer correlation with the experimental results has been observed in terms of SFC. The experimental UMA290 operating on 95RON gasoline returns 0.303 kg/kWh at 5250 rpm. This compares more closely than in prior studies with WAVE modelled values of 0.298 kg/kWh at 5500 rpm and 0.265 kg/kWh at 5000 rpm. The minimum modelled indolene SFC observed for the four-stroke 374 cm^3 engine was 0.240 kg/kWh at 5000 rpm.

With the ultimate objective of development of a HEV or RE-EV achieving ultra-low environmental impact initial modelling studies have explored lean operation on hydrogen. Indications are that almost zero emission operation may be possible. If possible, to be sustained, with such high air: fuel ratio operation, the engine could operate with extremely low environmental impact and maintain the state of charge of the vehicle battery system thereby countering the range anxiety problems still causing concern for BEVs. The low noise, vibration and harshness characteristics of stepped piston engines have already been presented [36]. Containment of a compact engine system within a semi-anechoic chamber would further reduce any remaining NVH challenges.

Engine production costs against comparable competing engines, whether of conventional two or four-stroke type, have consistently indicated significant savings. Studies against a direct injection four-stroke engine concluded that, on top of a 40%

investment cost reduction, a unit cost saving of 22% should be evident. Both the stepped piston and four-stroke engines were inline three-cylinder examples. The duplication of powertrain systems evident in HEVs and RE-EVs presents a serious challenge to product viability. Such significant engine cost reductions will naturally assist in overcoming this challenge.

Hydrogen fuelled engines have been shown to suffer from corrosion problems as has been discussed by Stępień [37] and Liu et al. [55]. The crossover system designed into stepped piston engines, to enable operation, is expected to offer advantage in countering the potential corrosion issues. The crossover essentially provides charge isolation from the moving mechanical components. The passageways forming the crossover systems are typically located within the crankcase casting and are completely separated from any other parts of the engine. This should provide additional protection from corrosion issues. Furthermore blow-by gases bypassing the combustion piston rings will only pass into the chamber system of the crossover rather than contaminating the areas of the engine that would suffer in conventional engines. Corrosion observed in other conventional hydrogen fuelled engines is not expected to present such problems with a stepped piston engine solution. The added advantages of two-stroke cycle operation, together with the complete separation of the lubrication methodology from the scavenging processes offers significant benefits in terms of durability, especially when compared with conventional two-stroke engines. Durability characteristics more typically associated with four-stroke engines has been regularly observed with stepped piston charged engines.

Exhaust gas recirculation (EGR) is inherent in two-stroke engines by virtue of their operating cycle. This occurs internally within the cylinder. External EGR could also be readily applied to the engine but has not yet been considered in the current research study.

Variable compression ratio technology, as demonstrated by the research of Turner et al. [29] and Blundell et al. [30] has been shown to offer further benefits in terms of performance and emissions reduction. This VCR technology could relatively easily be applied to the stepped piston engine due to the simplicity of the cylinder head and combustion chamber. Variable port timing methods could also provide further improvement, particularly away from the maximum power full load conditions. Variable port timing is also an effective method for providing an element of EGR control. No experimentation with VCR or variable port timing has been explored within this study but could provide a focus for further research.

5. Conclusion

Significant improvements to the simulated specific power and fuel consumption of the UMA290 stepped piston segregated scavenge engine have been presented operating on indolene/gasoline fuels. This research has been performed prior to planned hydrogen fuel modelling and operation to explore potential benefits of the engine type on low emission fuels for future HEVs or RE-EVs. Model predictions have indicated specific power output to date of 58.4 kW/litre using indolene compared with 61.1 kW/litre for the gasoline engine. The potential benefits, with

near zero emission operation possible, could counter the range anxiety still causing problems for electric vehicles. The approach should also counter the negative environmental impact that still exists for BEVs.

Acknowledgments: Realis Simulation/Ricardo are the developers of WAVE. Their assistance is gratefully acknowledged in allowing the simulation results presented.

Conflict of interest: The author declares no conflict of interest.

Notation

A_p	Knock multiplier
A_T	Activation temperature multiplier
B	Constant
C_m	Relative area scaling factor for heat transfer
C	Constant
c_1, c_2, c_3, c_4	FMEP constants
D	Cylinder bore diameter
e_T	Internal energy
h	Coefficient of heat transfer
k	Coefficient of thermal conductivity
l	Cylinder centre distance
N	Engine speed
O_N	Fuel research octane number
P	Instantaneous gas pressure
p	Pressure
p_{cyl}	Cylinder pressure
p_f	Friction means effective pressure
p_{max}	Maximum cylinder pressure
S	Stroke
t_i	Auto ignition start time
t_i	Time at commencement of end gas compression
t	Time
T	Instantaneous gas temperature
T_{unb}	Unburned gas temperature
U	Velocity
v_{ch}	Characteristic gas velocity
$x(\theta)$	Mass fraction burned at crank angle θ
θ	Crank angle
θ_0	Crank angle at the start of combustion
$\Delta\theta_b$	Duration of combustion
ρ	Density
μ	Dynamic viscosity
τ	Induction time

Abbreviations

1-d CFD	One dimensional computational fluid dynamic
4s 374	Four-stroke twin cylinder 374 cm^3 engine
BEV	Battery electric vehicle
BMEP	Brake mean effective pressure
CA50	Crank angle position for 50% of mass fraction burned
DI	Direct injection
DOHC	Double overhead cam
EC	Exhaust port closure
EO	Exhaust port opening
FMEP	Friction mean effective pressure
HEV	Hybrid electric vehicle
IC	Internal combustion
NO_x	Oxides of nitrogen
NVH	Noise vibration and harshness
PPM	Parts per million
RE-EV	Range extender electric vehicle
SPV580	Stepped piston V-4 580 cm^3 engine
SPX	Stepped piston crossover system
TC	Transfer port closure
TDC	Top dead centre
TO	Transfer port opening
UMA290	Stepped piston twin cylinder 290 cm^3 engine

References

1. Rauh N, Franke T, Krems JF. Understanding the Impact of Electric Vehicle Driving Experience on Range Anxiety. Human Factors: The Journal of the Human Factors and Ergonomics Society. 2014; 57(1): 177–187. doi: 10.1177/0018720814546372
2. Reitz RD, Ogawa H, Payri R, et al. IJER editorial: The future of the internal combustion engine. International Journal of Engine Research. 2019; 21(1): 3–10. doi: 10.1177/1468087419877990
3. Pevec D, Babic J, Carvalho A, et al. A survey-based assessment of how existing and potential electric vehicle owners perceive range anxiety. Journal of Cleaner Production. 2020; 276: 122779. doi: 10.1016/j.jclepro.2020.122779
4. Sobianowska-Turek A, Urbańska W, Janicka A, et al. The Necessity of Recycling of Waste Li-Ion Batteries Used in Electric Vehicles as Objects Posing a Threat to Human Health and the Environment. Recycling. 2021; 6(2): 35. doi: 10.3390/recycling6020035
5. Lipman TE, Maier P. Advanced materials supply considerations for electric vehicle applications. MRS Bulletin. 2021; 46(12): 1164–1175. doi: 10.1557/s43577-022-00263-z
6. Kalghatgi G. Is it the end of combustion and engine combustion research? Should it be? Transportation Engineering. 2022; 10: 100142. doi: 10.1016/j.treng.2022.100142
7. Requia WJ, Mohamed M, Higgins CD, et al. How clean are electric vehicles? Evidence-based review of the effects of electric mobility on air pollutants, greenhouse gas emissions and human health. Atmospheric Environment. 2018; 185: 64–77. doi: 10.1016/j.atmosenv.2018.04.040
8. Klimenko A. Aggregated toxicity of road vehicles as basis for future regulation in the field of atmospheric air protection. SN Applied Sciences. 2020; 2(12). doi: 10.1007/s42452-020-03874-w

9. European Union. Available online: https://www.consilium.europa.eu/en/press/press-releases/2023/12/18/euro-7-council-and-parliament-strike-provisional-deal-on-emissions-limits-for-road-vehicles/ (accessed on 19 August 2024).
10. Sterlepper S, Fischer M, Claßen J, et al. Concepts for Hydrogen Internal Combustion Engines and Their Implications on the Exhaust Gas Aftertreatment System. Energies. 2021; 14(23): 8166. doi: 10.3390/en14238166
11. Ravi SS, Osipov S, Turner JWG. Impact of Modern Vehicular Technologies and Emission Regulations on Improving Global Air Quality. Atmosphere. 2023; 14(7): 1164. doi: 10.3390/atmos14071164
12. Ravi SS, Brace C, Larkin C, et al. On the pursuit of emissions-free clean mobility—Electric vehicles versus e-fuels. Science of The Total Environment. 2023; 875: 162688. doi: 10.1016/j.scitotenv.2023.162688
13. Bassett M, Hall J, Kennedy G, et al. The Development of a Range Extender Electric Vehicle Demonstrator. SAE Technical Paper Series. 2013. doi: 10.4271/2013-01-1469
14. Milojević, S., Savić, S., Mitrović, S., et al. Solving the Problem of Friction and Wear in Auxiliary Devices of Internal Combustion Engines on the Example of Reciprocating Air Compressor for Vehicles. Tehnicki vjesnik—Technical Gazette. 2023; 30(1): 122–130. doi: 10.17559/tv-20220414105757
15. Milojević, S., Savić, S., Marić, D., et al. Correlation between Emission and Combustion Characteristics with the Compression Ratio and Fuel Injection Timing in Tribologically Optimized Diesel Engine. Tehnicki vjesnik—Technical Gazette. 2022; 29(4): 1210–1219. doi: 10.17559/tv-20211220232130
16. Milojević S, Glišović J, Savić S, et al. Particulate Matter Emission and Air Pollution Reduction by Applying Variable Systems in Tribologically Optimized Diesel Engines for Vehicles in Road Traffic. Atmosphere. 2024; 15(2): 184. doi: 10.3390/atmos15020184
17. Bukvić M, Gajević S, Skulić A, et al. Tribological Application of Nanocomposite Additives in Industrial Oils. Lubricants. 2023; 12(1): 6. doi: 10.3390/lubricants12010006
18. Milojevic S. Sustainable application of natural gas as engine fuel in city buses: Benefit and restrictions. Istrazivanja i projektovanja za privredu. 2017; 15(1): 81–88. doi: 10.5937/jaes15-12268
19. Wróbel K, Wróbel J, Tokarz W, et al. Hydrogen Internal Combustion Engine Vehicles: A Review. Energies. 2022; 15(23): 8937. doi: 10.3390/en15238937
20. Furuhama S, Kobayashi Y. Hydrogen Cars with LH_2-Tank, LH_2-Pump and Cold GH_2-lnjection Two-Stroke Engine. SAE transactions; 1982. pp. 1371–1383.
21. Caprioli S, Volza A, Mattarelli E, Rinaldini CA. High Performance and Near Zero Emissions 2-Stroke H2 Engine. SAE Technical Paper. 2023; 24: 0068.
22. Mattarelli E, Rinaldini CA, Marmorini L, et al. 2-Stroke RCCI Engines for Passenger Cars. Energies. 2022; 15(3): 1173. doi: 10.3390/en15031173
23. Volza A, Scrignoli F, Caprioli S, et al. Exploring the Potential of Hydrogen Opposed Piston Engines for Single-Cylinder Electric Generators: A Computational Study. SAE Technical Paper Series. 2023; 24: 128. doi: 10.4271/2023-24-0128
24. Karim GA. Hydrogen as a spark ignition engine fuel" (International Journal of Hydrogen Energy. 2023; 28(5): 569–577. doi: 10.1016/S0360-3199(02)00150-7
25. Verhelst S, Turner JWG. Hydrogen-Fueled Spark Ignition Engines. In: Tingas EA. (editor). Hydrogen for Future Thermal Engines. Green Energy and Technology. Springer, Cham; 2023.
26. Shinde BJ, Karunamurthy K. Recent progress in hydrogen fuelled internal combustion engine (H2ICE)—A comprehensive outlook. Materials Today: Proceedings. 2022; 51: 1568–1579. doi: 10.1016/j.matpr.2021.10.378
27. Cracknell R, Ciatti S, Dorofeev S, et al. Decarbonization of mobility, including transportation and renewable fuels. In: Proceedings of the Combustion Institute; 2023. pp.1–9.
28. Onorati A, Payri R, Vaglieco BM, et al. The role of hydrogen for future internal combustion engines. International Journal of Engine Research. 2022; 23(4): 529–540. doi: 10.1177/14680874221081947
29. Turner, J., Blundell, D., Pearson, R., et al. Project Omnivore: A Variable Compression Ratio ATAC 2-Stroke Engine for Ultra-Wide-Range HCCI Operation on a Variety of Fuels. SAE Paper. 2010; 1: 1249.
30. Blundell DW, Turner J, Pearson R, et al. The Omnivore Wide-range Auto-Ignition Engine: Results to Date using 98RON Unleaded Gasoline and E85 Fuels. SAE Technical Paper Series. 2010; 1: 0846. doi: 10.4271/2010-01-0846
31. Hooper PR. Low emission stepped piston engine for marine outboard motor application. In: Proceedings of the Institution of Mechanical Engineers; 2024.

32. Duret P, Ecomard A, Audinet M. A New Two-Stroke Engine with Compressed-Air Assisted Fuel Injection for High Efficiency low Emissions Applications. SAE Technical Paper Series. 1988
33. Schlunke K. (1989). The orbital combustion process engine. 10th Vienna Motorsymposium. VDI. 1989; 122: 63–68.
34. Shawcross D, Pumphrey C, Arnall D. A Five-Million Kilometre, 100-Vehicle Fleet Trial, of an Air-Assist Direct Fuel Injected, Automotive 2-Stroke Engine. SAE Technical Paper Series. 2000. doi: 10.4271/2000-01-0898
35. Hooper PR, Al-Shemmeri T, Goodwin MJ. Advanced modern low-emission two-stroke cycle engines. In: Proceedings of the Institution of Mechanical Engineers; 2011. pp. 1531–1543.
36. Hooper PR. Investigation into a stepped-piston engine solution for automotive range-extender vehicles and hybrid electric vehicles to meet future green transportation objectives. In: Proceedings of the Institution of Mechanical Engineers; 2017. pp. 305–317.
37. Stępień Z. A Comprehensive Overview of Hydrogen-Fueled Internal Combustion Engines: Achievements and Future Challenges. Energies. 2021; 14(20): 6504. doi: 10.3390/en14206504
38. Bernard Hooper Engineering Ltd. SPV580 engine data sheet. Available online: http://www.bernardhooperengineering.co.uk/spv580ds.htm (accessed on 28 September 2024).
39. Bernard Hooper Engineering Ltd. G290 engine data sheet. Available online: http://www.bernardhooperengineering.co.uk/g290ds.htm (accessed 28 September 2024).
40. Stone R. Introduction to Internal Combustion Engines, 4th ed. Macmillan Education UK; 2012.
41. Realis Simulation/Ricardo PLC. Available online: https://www.realis-simulation.com/products/wave/ (accessed on 20 August 2024).
42. Gajević S, Marković A, Milojević S, et al. Multi-Objective Optimization of Tribological Characteristics for Aluminum Composite Using Taguchi Grey and TOPSIS Approaches. Lubricants. 2024; 12(5): 171. doi: 10.3390/lubricants12050171
43. Hata N, Fujita T, Matsuo N. Modification of Two-Stroke Engine Intake System for Improvements of Fuel Consumption and Performance through the Yamaha Energy Induction System (YEIS). SAE Technical Paper Series. 1981. doi: 10.4271/810923
44. Hinds ET. Intake flow characteristics of a two-stroke cycle engine fitted with reed valves [PhD thesis]. Queen's University of Belfast; 1978.
45. Morrison JLM, Crossland B. An Introduction to the Mechanics of Machines, 2nd ed. Longman; 1971.
46. Wiebe I. Semi-empirical formula for combustion speed (German). In: Verlag der Akademie der Wissenschaften der UdSSR, Moscow; 1967.
47. Heywood JB, Sher E. The Two-Stroke Cycle Engine. Routledge; 2017.
48. Sher E. (1984) The Effect of Atmospheric Conditions on the Performance of an Airborne Two-Stroke Spark Ignition Engine. Proc. Inst. Mech. Eng. 1984; 198(15): 239–251.
49. Bird RB, Stewart WE, Lightfoot EN. Transport Phenomena, 2nd ed. Wiley; 2022.
50. Woschni G. A Universally Applicable Equation for the Instantaneous Heat Transfer Coefficient in the Internal Combustion Engine. SAE Technical Paper Series. 1967. doi: 10.4271/670931
51. Chen SK, Flynn PF. Development of a Single Cylinder Compression Ignition Research Engine. SAE Technical Paper Series. 1965. doi: 10.4271/650733
52. Douaud AM, Eyzat P. Four-Octane-Number Method for Predicting the Anti-Knock Behavior of Fuels and Engines. SAE Technical Paper Series. 1978. doi: 10.4271/780080
53. SAE Standard J1349. Engine Power Test Code—Spark Ignition and Compression Ignition—Net Power Rating. SAE International, Warrendale, PA; 1995.
54. Hooper B, Favill JE. Modern Stepped Piston Engines. In: Proceedings of Design and Development of Small IC Engines Conference; 31 May–2 June 1978. IMechE paper C133/78.
55. Liu Z, Guo Z, Rao X, et al. A comprehensive review on the material performance affected by gaseous alternative fuels in internal combustion engines. Engineering Failure Analysis. 2022; 139: 106507. doi: 10.1016/j.engfailanal.2022.106507.